

MOMENTUM TRANSFER IN MAN-MADE EMBAYMENTS AT LOW WATER DEPTH

Yoshihisa Kawahara*, Muhammad A. JALIL**, Nobuyuki Tamai*

* Dept. of Civil Engineering, University of Tokyo, Bunkyo-ku, Tokyo 113, Japan

** Dept. of Civil Engineering, Bangladesh University of Engineering & Technology, Dhaka-1000, Bangladesh

Abstract

Construction of man-made embayments in riparian areas to provide natural friendly environment have attracted an increasing interest in Japan. In this study, experimental and numerical studies were carried out to clarify the momentum transfer process in embayments of various entrance shape under low water steady flow conditions. Velocity measurement showed that while the mixing layer along the embayment - main channel interface and the recirculation pattern in embayments change considerably depending on the hydraulic conditions, time averaged velocity shows little variation in magnitude and flow direction over the flow depth. Hence, a numerical model based on shallow water equations incorporated with the depth-averaged $k - \epsilon$ model was developed for the analysis of depth-averaged velocity field. It was confirmed that the numerical model can yield the mean velocity distributions in good agreement with experimental data.

1 Introduction

River improvement works using conventional engineering methods may destroy the natural healthy environment in riparian areas and cause adverse effects on the ecosystem. In order to avoid monotonous artificial environment and to preserve high level of natural condition in riparian areas, construction of embayments along the shore of rivers which are able to provide shelters, foods and nutrients for ecosystem is highly needed.

Embayments along a river bank are basically dead water zones. Such zones not only occur frequently in small dimension in natural rivers with irregular side and bed configuration, but also in large dimension in streams passing groynes, bays and harbors. In all the cases, the mass exchange between the dead water zone and the main stream is of prime importance because it controls the water quality of both regions. Typical properties characterizing this quality are concentration of chemical substances, biodegradable organic matter, dissolved oxygen or micro-organisms and so on. Hence, prior to actual construction of man-made embayments, quantitative evaluations of specific properties in an embayment are essential. These require a sufficient knowledge of the flow characteristics in the embayment and at its entrance.

The flow in an embayment is complex because of separation, recirculation, complex eddy structures, high turbulence intensities and forced oscillation for low flow

condition. Owing to the complexity of the flow, only a few studies have been reported on mean velocity field in similar geometric configuration (Westrich-Clad(1979), Booij(1991), Tingsanchali-Chinanont(1991), Langendoen(1992)). Evidently, the complexity increases for flood flow. The understanding of characteristics of flood flows are highly important to take measures for maintaining the functions of embayments.

The present study focuses on the flow characteristics at low water depth. Its objectives are (1) to present the results of detailed measurement on mean velocity distribution in embayments of different entrance shape, and (2) to show the applicability of the numerical model to the mean flow in embayments.

2 Experimental Setup and Conditions

Experiments were carried out in a 100 cm wide tilting flume that has a compound cross section (Fig. 1). The embayment built up in the flume has the size 20 cm × 20 cm in plan and the depth 5.2 cm equal to the height of the flood plain. The bed slope of the flume was set at 1/2,000 for all the experiments. More than 10 types of the embayment were tested as a series of this experiment. Table 1 shows some of them which will be explained here. The plate introduced along the channel-embayment interface to block the opening of the embayment was 1.4 cm thick. The measuring stations were mainly concentrated in and around embayments.

Water depth was measured by point gauge. The distributions of longitudinal and transverse velocity components were measured by a two component electromagnetic currentmeter. The probe of the currentmeter is 5 mm in diameter and 1.8 cm in length. The measurements were started after the establishment of a steady state flow in the channel.

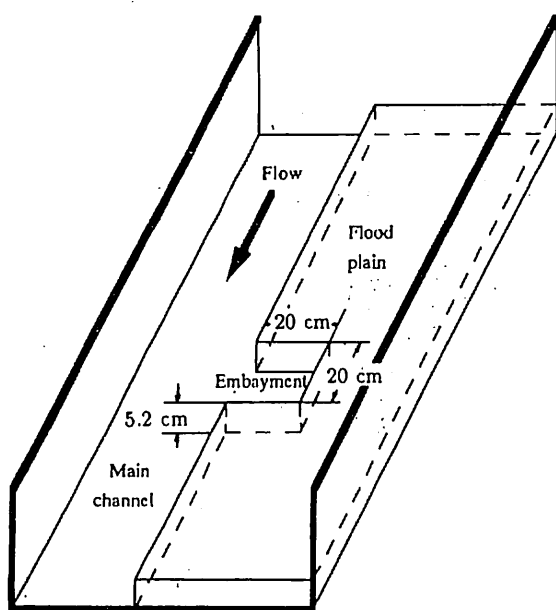
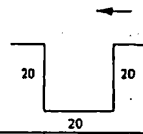
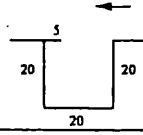
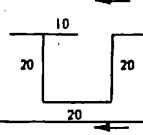
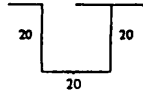


Fig. 1 Perspective view of the test section.

Table 1 Experimental conditions.

Expt. no.	Geometry of Embayment (dimensions are in cm)	Discharge (l/s)	Flow depth in main channel (cm)	Average velocity in main channel (cm/s)	Water depth in embayment (cm)	Reynolds number
1		5.93	4.69	32.28	4.63	12200
2		3.50	3.54	25.25	3.54	7600
3		3.34	3.50	24.36	3.45	7200
4		3.28	3.44	24.31	3.38	7100

3 Numerical Model

3.1 Basic Equations

The turbulent flows in and around embayments are unsteady and three-dimensional. However, the three-dimensionality is of secondary importance in our cases because mean velocity distribution is nearly uniform over the flow depth, judging from the experimental results as will be shown later. Hence the present numerical model reduces to a two-dimensional one, which can be a practical tool for the flow analysis.

The basic equations based on the depth-averaged approach can be written as follows:

$$\frac{\partial h}{\partial t} + \frac{\partial hu}{\partial x} + \frac{\partial hv}{\partial y} = 0 \quad (1)$$

$$\frac{\partial hu}{\partial t} + \frac{\partial \beta_{uu} hu^2}{\partial x} + \frac{\partial \beta_{uv} huv}{\partial y} = -gh \frac{\partial z_s}{\partial x} + \frac{1}{\rho} \left(-\tau_{bx} + \frac{\partial hT_{xx}}{\partial x} + \frac{\partial hT_{xy}}{\partial y} \right) \quad (2)$$

$$\frac{\partial hv}{\partial t} + \frac{\partial \beta_{uv} huv}{\partial x} + \frac{\partial \beta_{vv} hv^2}{\partial y} = -gh \frac{\partial z_s}{\partial y} + \frac{1}{\rho} \left(-\tau_{by} + \frac{\partial hT_{xy}}{\partial x} + \frac{\partial hT_{yy}}{\partial y} \right) \quad (3)$$

where h = water depth, u, v = depth-averaged longitudinal and transverse velocity components, z_s = water level, τ_{bx}, τ_{by} = bottom shear stresses, T_{ij} = depth-averaged turbulent shear stresses and β_{ij} = momentum correction factors. Since the measured velocity distribution is nearly uniform over the flow depth, the values of β_{ij} were set to unity in this study. The bottom shear stresses can be expressed as,

$$\frac{\tau_{bx}}{\rho} = u_*^2 \frac{u}{\sqrt{u^2 + v^2}}, \quad \frac{\tau_{by}}{\rho} = u_*^2 \frac{v}{\sqrt{u^2 + v^2}}, \quad u_* = \sqrt{c_f (u^2 + v^2)} \quad (4)$$

where c_f is a friction coefficient. The turbulent stresses were determined using the depth-averaged $k - \epsilon$ model of Rastogi-Rodi(1978), where the depth-averaged turbulent shear stresses are given as follows:

$$\frac{T_{ij}}{\rho} = \nu_t \left(\frac{\partial u_i}{\partial x_j} + \frac{\partial u_j}{\partial x_i} \right) - \frac{2}{3} k \delta_{ij}, \quad \nu_t = c_\mu \frac{k^2}{\epsilon} \quad (5)$$

The distribution of turbulence energy k and its dissipation rate ϵ were obtained from the transport equations.

$$\frac{\partial hk}{\partial t} + \frac{\partial}{\partial x}(uk) + \frac{\partial}{\partial y}(vk) = \frac{\partial}{\partial x} \left(\frac{\nu_t}{\sigma_k} \frac{\partial k}{\partial x} \right) + \frac{\partial}{\partial y} \left(\frac{\nu_t}{\sigma_k} \frac{\partial k}{\partial y} \right) + P_{kh} + P_{kv} - \epsilon \quad (6)$$

$$\frac{\partial h\epsilon}{\partial t} + \frac{\partial}{\partial x}(u\epsilon) + \frac{\partial}{\partial y}(v\epsilon) = \frac{\partial}{\partial x} \left(\frac{\nu_t}{\sigma_\epsilon} \frac{\partial \epsilon}{\partial x} \right) + \frac{\partial}{\partial y} \left(\frac{\nu_t}{\sigma_\epsilon} \frac{\partial \epsilon}{\partial y} \right) + P_{\epsilon h} + P_{\epsilon v} - c_{2\epsilon} \frac{\epsilon^2}{k} \quad (7)$$

$$P_{kh} = \nu_t \left[2 \left(\frac{\partial u}{\partial x} \right)^2 + 2 \left(\frac{\partial v}{\partial y} \right)^2 + \left(\frac{\partial u}{\partial y} + \frac{\partial v}{\partial x} \right)^2 \right], \quad P_{kv} = c_k \frac{u_*^3}{h} \quad (8)$$

$$P_{\epsilon h} = c_{1\epsilon} \left(\frac{\epsilon}{k} \right) P_{kh}, \quad P_{\epsilon v} = c_\epsilon \frac{u_*^4}{h^2}, \quad c_k = \frac{1}{\sqrt{c_f}}, \quad c_\epsilon = 3.6 \frac{c_{2\epsilon}}{c_f^{3/4}} \quad (9)$$

where the model constants have the values $c_\mu = 0.09, c_{1\epsilon} = 1.44, c_{2\epsilon} = 1.92, \sigma_k = 1.0, \sigma_\epsilon = 1.3$.

3.2 Numerical Procedures

The continuity equation and two momentum equations were solved using a rigid lid approximation, i.e., the water surface slope terms in the shallow water equations are replaced by pressure terms. The converged solution to the set of elliptic equations was obtained using the SIMPLE algorithm. Simultaneous algebraic equations were solved using MSI (Modified Strongly Implicit) procedure.

Boundary conditions must be specified for all the variables around the whole flow domain. Across the channel inflow boundary, specified values of all the variables were prescribed. The velocity values were taken from experiments. The values of k and ϵ were calculated assuming the fully developed condition. Along the solid boundaries, because of the steep variation in flow properties close to the walls, a fine grid would normally be required. To avoid this, the "wall function technique" has been used for u, v, k, ϵ assuming the existence of a log-law velocity profile and the local equilibrium for turbulence energy at the nodal points adjacent to the solid boundaries. The value of zero was employed for the normal velocity component and the normal pressure gradient at the wall. At the outlet, the streamwise gradients of all the variable were set to zero.

Since the computer code utilized the power law scheme for advection terms, the grid dependency of the converged solution was examined to determine the resolution of the grid system. The calculations shown here were done on the grid whose maximum size is 1.0 cm.

4 Results and Discussions

The experimental and numerical results are presented and compared with each other in this section.

4.1 Case-1

The interface is completely open in this case. Fig. 2 shows the flow patterns at the three different levels designated as z_1, z_2 and z_3 planes which located at 30 %, 50 % and 80 % of the water depth from the bottom. The general flow pattern in each plane is almost the same over a large portion of the embayment. However, we can notice the existence of secondary current i.e., the velocity vectors change their direction over the flow depth although the secondary current is very weak.

A square grid with 20×20 grid points in the embayment was used in the computation. The predicted flow pattern shown in Fig. 3 agrees very well with the measured flow field. In Fig. 4 the longitudinal and transverse velocity components are compared along the bisectors which pass the center of the embayment. Clearly the components are predicted very well.

4.2 CASE-2

The interface was 25 % blocked from the downstream side in this case. The flow pattern is depicted in Fig. 5(a). This particular geometry of the interface changes the

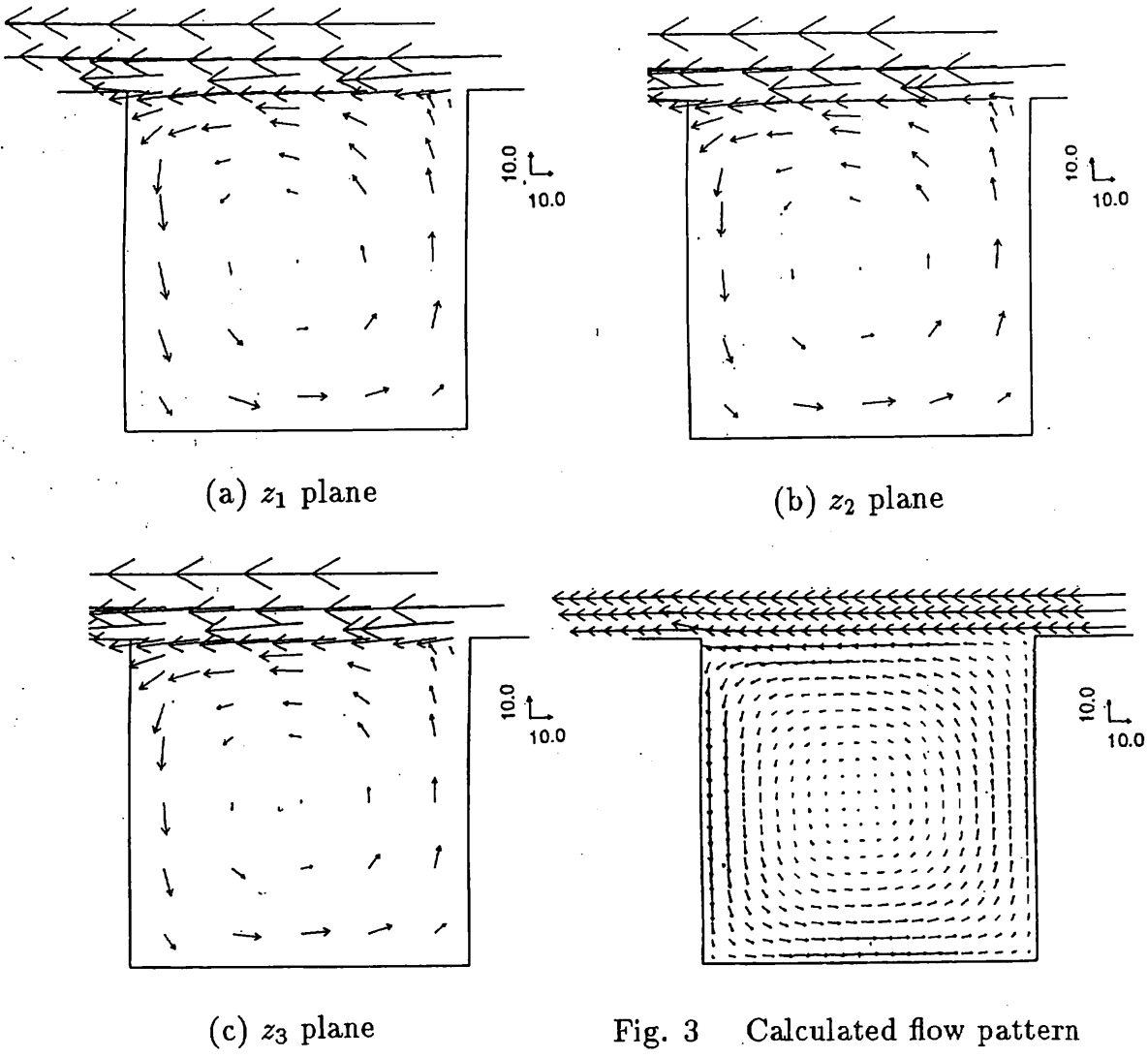


Fig. 2 Flow pattern for Case-1.

Fig. 3 Calculated flow pattern for Case-1.

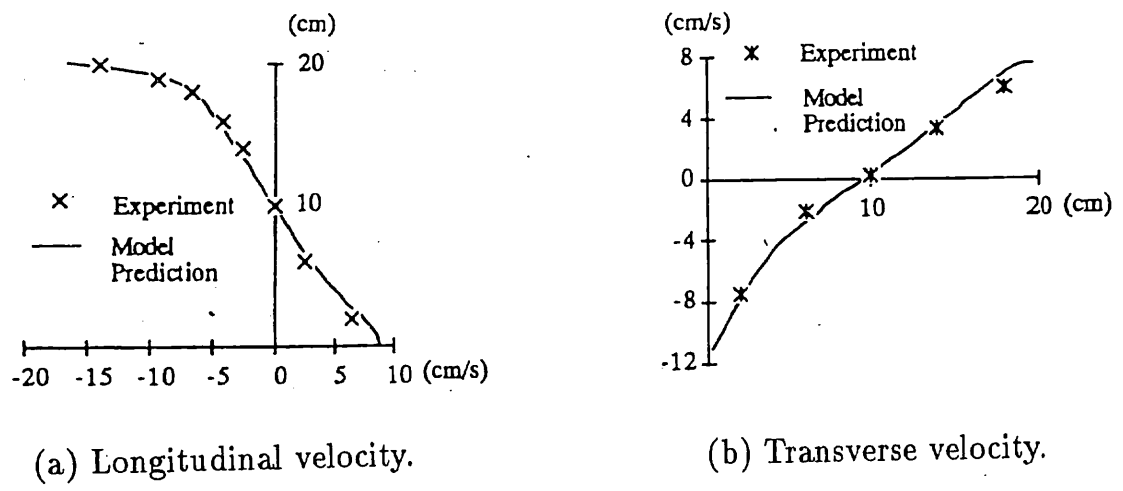


Fig. 4 Comparison of velocity profiles for Case-1.

flow pattern considerably. Two gyres are developed in the embayment - one is large and the other is much smaller. The larger anticlockwise gyre fills the embayment completely except the N-W corner where the smaller gyre is set in the clockwise direction.

The predicted flow pattern is displayed in Fig. 5(b). It is apparent that the computed velocity field has two recirculation zones which is in agreement with the measured velocity field, i.e., the velocity pattern has been faithfully reproduced by the model. However, the relative position of the large recirculation zone, and the magnitude and direction of the velocity vectors over the whole embayment as computed by the model are not in very good agreement with the measured data. This is due to the disturbance of flow field generated by wind because the flume is setup outside the building.

4.3 CASE-3

Drastic change in the flow pattern occurs when the interface is blocked by 50 % from the downstream side (Fig. 6(a)). One small anticlockwise gyre is set near the open interface and another relatively large gyre is formed in the remaining zone of the embayment. The smaller gyre is circular in shape. The larger gyre is somewhat triangular in shape with its center located much downstream of the embayment center and away from the main channel. In each gyre, the velocity decreases in the direction of the recirculation. This two gyre system was also observed by Westrich-Clad(1979).

The computed velocity field is displayed in Fig. 6(b). It is observed that the presence of two recirculation zones in the embayment and their relative positions have been correctly captured by the numerical model. However, there are some disagreement between the two results in greater details, which is also due to the flow disturbance by wind during the measurement.

4.4 CASE-4

In this experiment, the interface was 50 % open in the downstream side. The flow pattern is shown in Fig. 7(a). It is observed that one relatively small clockwise gyre is developed in the N-E corner of the embayment and another anticlockwise large gyre is formed in the remaining zone of the embayment. The center of the large gyre is nearer to the upstream cross wall and the main channel. The velocity decreases in the direction of the large gyre. The shape of the large gyre is somewhat rectangular.

Fig. 7(b) shows the calculated flow pattern. It is seen that the agreement between them is not so good. Although the numerical model captures the central gyre, it fails to reproduce the small gyre at the N-E corner of the embayment. The presence of the small gyre is probably the result of strong wind action on the flow field during the measurement. Also the center of the large gyre is shifted to the upstream being driven by the wind. Hence a satisfactory quantitative agreement between the measured and computed velocity patterns should not be expected.

The flow visualization using aluminum powder with light sheet technique was made to capture the flow features along the interface and in the embayment. The development of a row of vortices and the mass transfer along the interface were discusses in Jalil et

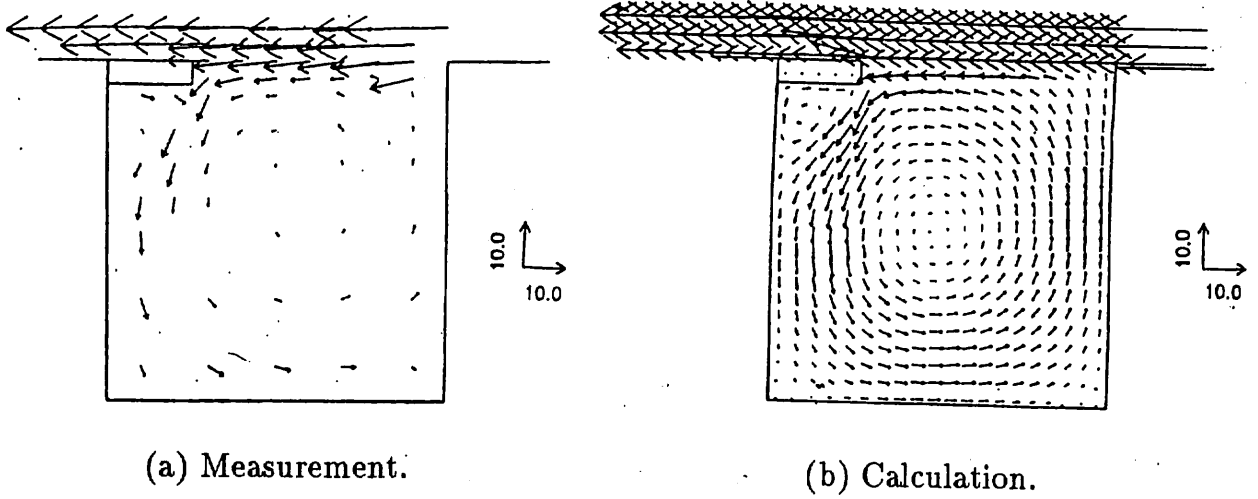


Fig. 5 Comparison of flow pattern for Case-2.

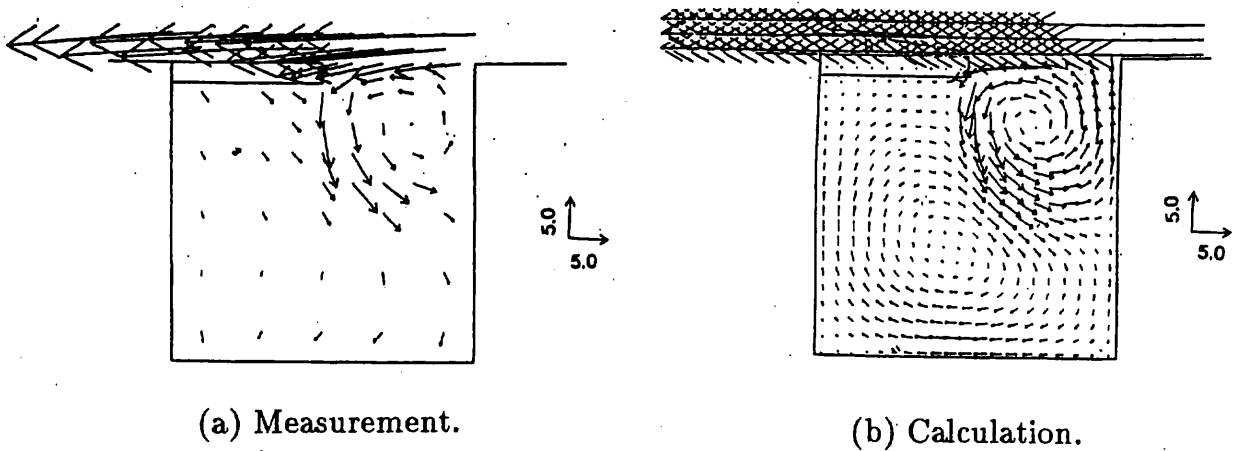


Fig. 6 Comparison of flow pattern for Case-3.

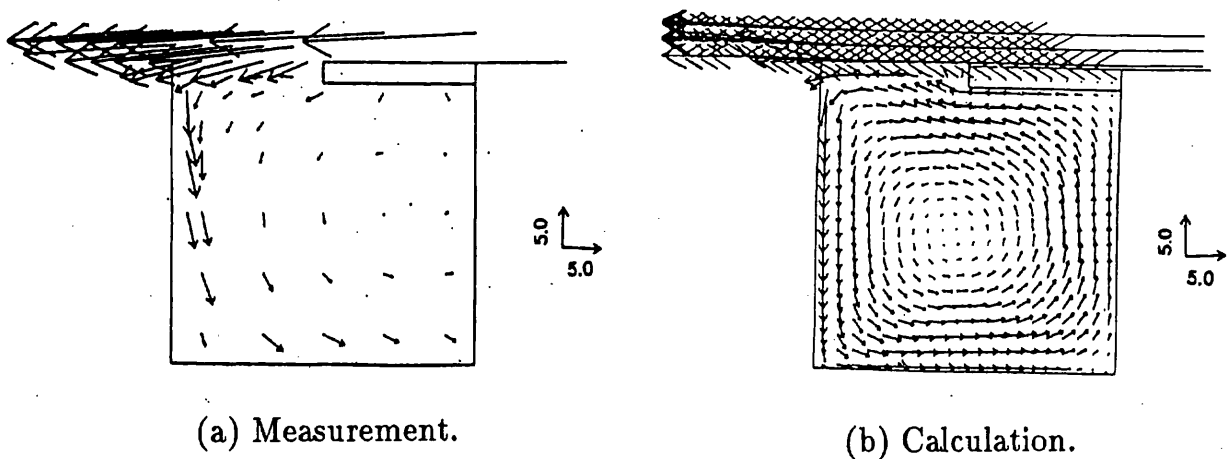


Fig. 7 Comparison of flow pattern for Case-4.

al. (1990).

5 Conclusions

The following conclusions can be drawn from the present study.

1. The geometry of an embayment has considerable influence on the flow characteristics, such as the number, size and position of gyres in the embayment and at its entrance.
2. The mean flow is nearly two-dimensional over a large portion of the embayment when the water depth is small and depth-averaged calculation is justifiable.
3. The proposed numerical model is capable of predicting the velocity field very well when the embayment is of square shape regardless of the opening ratio of the interface and the opening position.

Acknowledgement

The authors gratefully acknowledge the assistance of Dr. Tu, Mr. Nakagawa and Mr. Taishi in conducting the experiments reported here. The study was partly supported by the Maeda Memorial Foundation for Engineering and the Foundation for River Environment Management.

References

1. Booij, R.: Eddy viscosity in a harbour, Proc. XXIV IAHR Congress, Madrid, Vol.C, 81-90 (1991).
2. Jalil, M. A., Kawahara, Y., Tamai, N. and Kan, K.: Experimental investigation of flow in embayment, J. Hydraulic Eng., JSCE, 37, 503-510 (1994).
3. Langendoen, E. J.: Flow patterns and transport of dissolved matter in tidal harbours, Report No. ISSN 0169-6548, Delft University of Technology (1992).
4. Rastogi, A.K. and Rodi, W.: Predictions of heat and mass transfer in open channels, J. Hydraulics Div., ASCE, Vol.104, HY3, 397-420 (1978).
5. Tingsanchali, T. and Chirananont, B.: Investigation of flow circulation in a channel side pool, Proc. International Conference on Environmental Hydraulics, Vol.1, 467-472 (1991).
6. Westrich, B. and Clad, A.: Mass and heat exchange in flows with recirculating zones, Proc: IAHR Congress on Hydraulic Engineering in Water Resources Development and Management, Vol.3, 269-276 (1979).